Effect of Cu(NO$_3$)$_2$ and Cu(CH$_3$COO)$_2$ Activating Additives on Combustion Characteristics of Anthracite and Its Semi-Coke

Kirill Larionov [1,2,*], **Konstantin Slyusarskiy** [1,2], **Svyatoslav Tsibulskiy** [1], **Anton Tolokolnikov** [1], **Ilya Mishakov** [2,3], **Yury Bauman** [2,3], **Aleksey Vedyagin** [2,3] **and Alexander Gromov** [2]

1   School of Energy & Power Engineering, National Research Tomsk Polytechnic University, 634050 Tomsk, Russia; konstantinsv@tpu.ru (K.S.); stzibulsky@tpu.ru (S.T.); aat18@tpu.ru (A.T.)
2   Laboratory of Catalysis and Processing of Hydrocarbons, National University of Science and Technology "MISIS", 119049 Moscow, Russia; mishakov@catalysis.ru (I.M.); bauman@catalysis.ru (Y.B.); vedyagin@catalysis.ru (A.V.); a.gromov@misis.ru (A.G.)
3   Department of Materials Science and Functional Materials, Boreskov Institute of Catalysis SB RAS, 630090 Novosibirsk, Russia
*   Correspondence: larryk@tpu.ru; Tel.: +7-3832-701-777 (ext. 1609)

check for updates

Abstract: The process of anthracite and its semi-coke combustion in the presence of 5 wt.% (in terms of dry salt) additives of copper salts Cu(NO$_3$)$_2$ and Cu(CH$_3$COO)$_2$ was studied. The activating additives were introduced by an incipient wetness procedure. The ignition and combustion parameters for coal samples were examined in the combustion chamber at the heating medium temperatures (T_g) of 600–800 °C. The composition of the gaseous combustion products was controlled using an on-line gas analyzer. The fuel modification with copper salts was found to reduce the ignition delay time on average, along with a drop in the minimum ignition temperature T_{min} by 138–277 °C. With an increase in T_g temperature, a significant reduction in the ignition delay time for the anthracite and semi-coke samples (by a factor of 6.7) was observed. The maximum difference in the ignition delay time between the original and modified samples of anthracite (ΔT_i = 5.5 s) and semi-coke (ΔT_i = 5.4 s) was recorded at a T_g temperature of 600 °C in the case of Cu(CH$_3$COO)$_2$. The emergence of micro-explosions was detected at an early stage of combustion via high-speed video imaging for samples modified by copper acetate. According to the on-line gas analysis data, the addition of copper salts permits one to reduce the volume of CO formed by 40% on average, providing complete oxidation of the fuel to CO$_2$. It was shown that the introduction of additives promoted the reduction in the NO$_x$ emissions during the combustion of the anthracite and semi-coke samples.

Keywords: anthracite; semi-coke; ignition; combustion; activating additive; copper acetate; copper nitrate

1. Introduction

Coal is considered as one of the main pollution sources worldwide [1]. Despite this, its significant share in both the primary energy (more than 25%) and, especially, electricity generation (around 35%) [2] makes it impossible to avoid using coal technology in the upcoming decades. That is why improving the existing technologies has attracted much interest during recent years. While the application of anthracite for power generation is characterized by higher pollutant emissions [3], its combustion has been thoroughly studied recently [4–6]. The catalytic combustion process is a viable technology for the low reactivity fuels [4,5,7,8], like anthracite, which permits one to increase the effectiveness of the fuel conversion [4,9] and enhance the environmental characteristics of the corresponding equipment [1,10].

The catalytic properties of different metals (predominantly, alkali and alkali-earth metals) have been extensively studied during recent decades [6,11–15]. The experimental character of such studies is caused by the complexity of the coal structure and the processes taking place during coal heating [16], which are too complex to precisely simulate. The major contribution to the research on the effect of transitional metals (using Ce and Fe oxides) in different forms on the combustion of anthracite and some other coals was made by Gong et al. [5,7,8,17,18]. The significant promoting effect of CeO_2 and Fe_2O_3 on the combustion of different coals (predominantly based on the thermal analysis data) was reported [6,7,11]. The action mechanism of the activating additive proposed in [7,13] is based on an assumption of consecutive oxidation and reduction reactions of metal oxide. The more significant catalytic effect of CeO_2 and Fe_2O_3 was observed for the samples with higher fixed carbon content [5], indicating that their application, together with high-quality coals, is more effective. In addition, some researches were performed using oxides of La [14], Mn [4], Zn [19], Cu [20,21], but only the latter was found to have a considerable effect on the combustion process. The use of the metal oxide precursors instead of oxides themselves was found to have an even stronger effect [20,21], as, for example, in the case of the copper oxide precursor [20].

At the same time, the unexpected effects could appear under the conditions of real equipment due to different chemical reactions occurring at high heating rates [4,22] and possible interactions between the ash components and promoting additives [8,18,21,23]. While the general regularities of thermogravimetry could be projected on actual equipment and processes to improve the applicability of results, the advanced experimental technics had been utilized recently [4,15,24,25]. This allowed for getting new insights on the mechanism of combustion promotion with the activating additives.

A study on the oxidation of anthracite modified with the copper oxide precursor additive under the conditions of the thermal analyzer was recently reported [20]. However, as mentioned earlier, the thermal analysis does not allow for obtaining the results relevant to the further application. The present research is focused on the investigation of the effect that the copper oxide precursors might have on the combustion of anthracite and its semi-coke at conditions similar to the real anthracite-fired equipment.

2. Materials and Methods

2.1. Preparation and Characterization of the Samples

The initial samples studied in the present work were anthracite (further referred to as 'A') from the Krasnogorsk deposit of the Kemerovo region and semi-coke (designated as 'SC') obtained after its pyrolytic treatment [26]. Firstly, a sample of anthracite (with a particle size of 5–10 mm) was ground in a rattler in the following grinding mode: the mass ratio of grinding bodies to the material was 1:1, and the grinding time was 8 h. The grinding procedure was followed by the screening to get the fraction with a size < 80 μm. Then, a part of the obtained anthracite powder was subjected to pyrolytic heating in a rotating reactor with a constant purging with an inert gas (argon) at 650 °C (heating rate of 10 °C/min) for 3 h. The proximate analysis (moisture, ash, volatile matter content, and calorific value) was performed according to the ISO standardized methods: ISO 589: 2008 "Hard coal—Determination of total moisture"; ISO 1171: 2010 "Solid mineral fuels—Determination of ash"; ISO 562: 2010 "Hard coal and coke—Determination of volatile matter"; and ISO 1928: 2009 "Solid mineral fuel. Determination of gross calorific value and calculation of net calorific value". The obtained characteristics are presented in Table 1.

The proximate analysis results of the anthracite and semi-coke samples reveal high values of the ash content of 17.7 and 21.4 wt.%, respectively. The anthracite sample volatile matter content (7.2 wt.%) exceeds the average values typical for the fuels with such a high coalification degree. The pyrolytic processing of the initial sample reduces this value to 1.7 wt.%.

Table 1. Characteristics of the anthracite (A) and its semi-coke (SC) samples.

Characteristic	A	SC
Moisture content W [a], wt.%	2.1	0.7
Ash content A [d], wt.%	17.7	21.4
Volatile matter content V [daf], wt.%	7.2	1.7
Net heating value, MJ/kg	24.8	26.2

Indexes a, d, and daf are analytical, dry and dry-ash-free mass of the sample.

Samples A and SC are also different in particle morphology, as can be seen from the micrographs shown in Figure 1. The images were obtained using a JSM-6460LV scanning electron microscope (JEOL, Japan) with a focused ion beam.

×1000

(**a**)　　　　　(**b**)

×3000

(**c**)　　　　　(**d**)
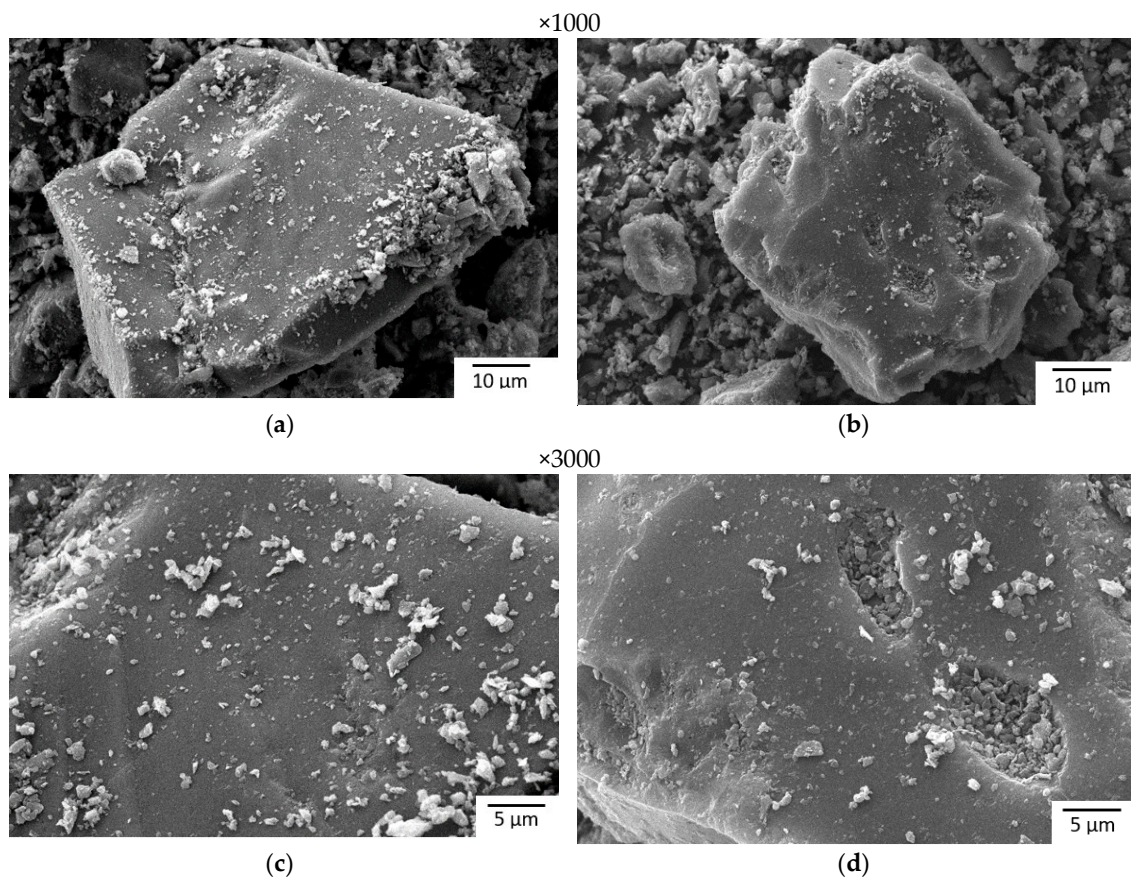
Figure 1. SEM images of the initial anthracite and semi-coke samples: (**a,c**)—sample A; (**b,d**)—sample SC.

The studied samples consist of faceted particles of an irregular shape with a monolithic surface containing a number of smaller fragments less than 5 μm in size. It is important to note that the SC sample (Figure 1b,d) has a more heterogeneous surface with various cavities and cracks, whose formation can be associated with the removal of volatile compounds (Table 1) during the pyrolytic treatment of anthracite.

2.2. Introduction of the Activating Additives

The crystalline hydrates $Cu(NO_3)_2 \cdot 3H_2O$ and $Cu(CH_3COO)_2 \cdot H_2O$ were used as precursors. The modification of the sample with salt was performed by an incipient wetness impregnation procedure described elsewhere [27,28]. This method was proven to provide a rather uniform distribution of the additive over the surface of the fuel's powder particles [27]. The content of the activating additive was 5 wt.% (in terms of dry salt) for all the samples. The reference samples (without additives) were

subjected to the same procedures using distilled water instead of aqueous solutions of salt and dried. This allowed us to conduct the same processing steps as in the case of modified samples.

The chemical composition of all the studied samples, including ash content, was determined using an elemental analyzer Euro EA 3000 (EuroVector, Italy). The results are given in Table 2. Here and throughout, the samples appear in the text according to their tags.

Table 2. List of the synthesized samples, their designations and chemical compositions.

Type and Content of Additive	Tag	Elemental Composition [1], wt.%							Ash Content A [1], wt.%
		C	H	N	S	O	H/C	O/C	
Anthracite									
No additive	A	69.9	1.4	1.2	0.2	9.6	0.24	0.09	17.7
5 wt.% $Cu(NO_3)_2$	A/1	62.8	1.4	2.1	0.2	13.4	0.27	0.16	20.1
5 wt.% $Cu(CH_3COO)_2$	A/2	64.4	1.7	1.0	0.1	12.9	0.32	0.15	19.9
Anthracite Semi-Coke									
No additive	SC	73.8	1.0	1.1	0.1	2.6	0.16	0.03	21.4
5 wt.% $Cu(NO_3)_2$	SC/1	68.6	1.1	1.7	0.1	5.0	0.19	0.05	23.4
5 wt.% $Cu(CH_3COO)_2$	SC/2	67.5	1.5	0.9	0.1	6.0	0.27	0.07	24.0

[1] in relation to the mass of a dry sample.

A certain increase in the ash content was observed for all the modified samples due to the copper oxide formation resulted from the sample combustion. The increase in ash content when using the studied additives of copper salts was 2.1–2.6 wt.%.

The O/C ratio was also found to be increased by 1.5–2.5 times for all the modified samples. For the anthracite samples, the O/C ratio was higher than for the semi-coke samples due to the removal of oxygen-containing species during the pyrolysis [29,30]. According to the data in Table 2, for the modified samples, an increase in the H/C ratio could be observed. For modified samples, its value was 1.1–1.6 times higher than for the original samples of anthracite and semi-coke.

The apparent growth in the nitrogen content for the samples modified with $Cu(NO_3)_2$ can be explained by the nature of the used additive [31].

2.3. Combustion Experiments

The ignition and combustion characteristics of the fuel samples were studied using an experimental setup schematically shown in Figure 2.

The setup comprises a combustion chamber, a high-speed video camera, an on-line gas analyzer, and a coordinate mechanism with a movable sample holder. The TSMP Ltd. R14-U furnace with a temperature controller was used as a combustion chamber. The Fastcam CA4 5 (Photron, San Diego, CA, USA) camera was applied for the process imaging. The recording procedure was performed with a 1024 × 1024 resolution at a frame rate of 105 fps. The holder of the coordinate mechanism was adjusted to stop in the center of the furnace where the temperature was equal to the preset value.

For the study, a specimen of ~0.1 ± 0.01 g was loaded in a cylindrical cup. Then the cup was placed upside down on the holder of the coordinate mechanism and removed. The small pile of the sample of a conical form obtained by this procedure was left on the holder of the coordinate mechanism. The experimental procedure consisted of a few consecutive stages. In a temperature-controlled furnace, the required temperature of the heating medium was preset (in a range of 600–800 °C with an intermediate step of 50 °C) and controlled using a chromel–alumel thermocouple. In the beginning, the fuel was located on the sample holder. Then the coordinate mechanism was launched via PC, and the sample was supplied into the furnace. The recording procedure was started at the moment when the sample crosses the internal wall of the furnace. The gas-phase combustion products were removed into the ventilation system. The on-line gas analyzer was used to define the composition of the outlet gases.
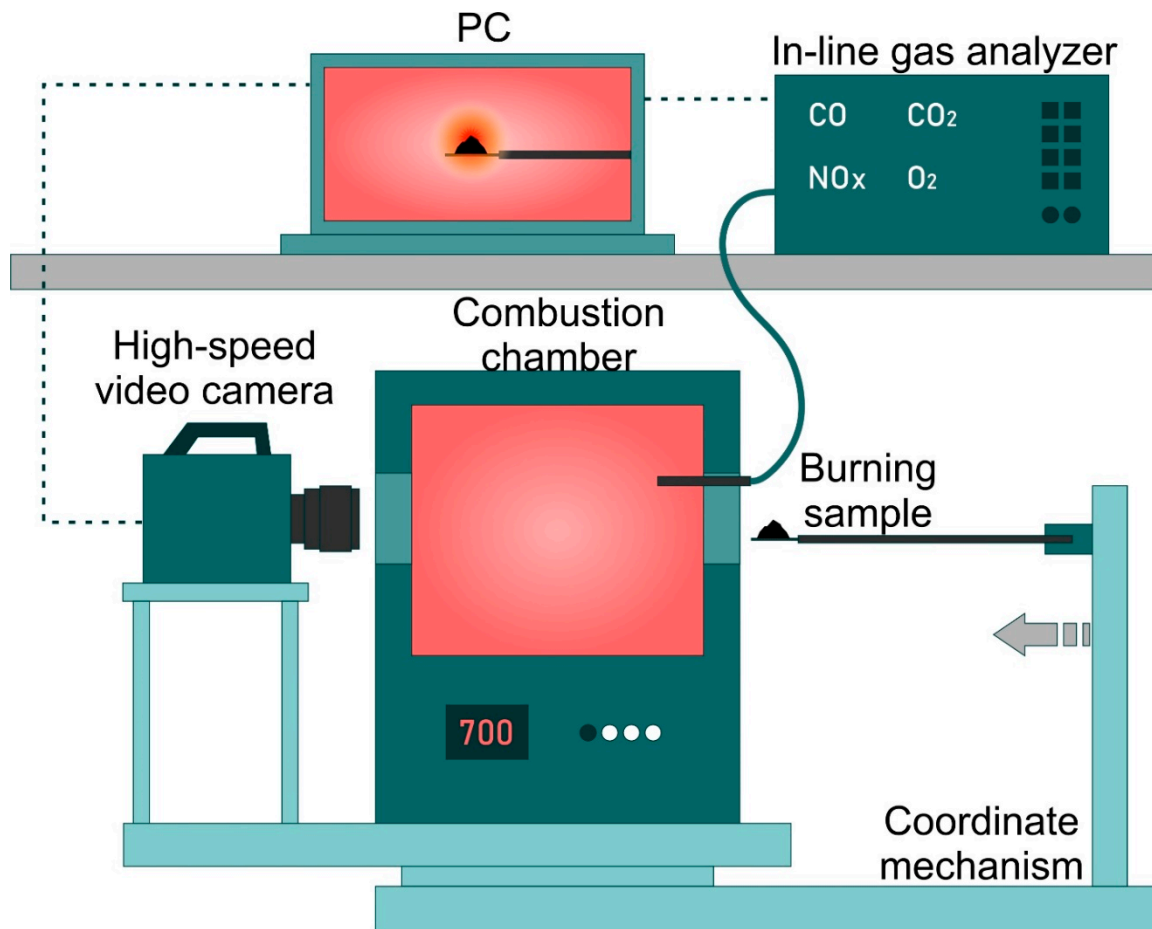
Figure 2. Experimental setup for studying the combustion process of the solid fuels.

A comparative assessment of the ignition process characteristics at different temperatures of the heating medium was carried out by analyzing the ignition delay time recorded by means of a high-speed video camera. The ignition delay time was considered to be the time from the moment when the holder with the fuel sample entered the focus of the video camera to the beginning of the visible glow on the fuel surface, which corresponds to the beginning of the combustion stage. At least 5 parallel experiments were carried out under the same conditions for each sample under study.

2.4. Determination of the Minimum Ignition Temperature

The minimum ignition temperature T_{min} was determined as the lowest temperature of the heating medium, at which the ignition of the fuel sample takes place. The procedure was as follows: the sample was supplied into the furnace and exposed for 1 min. The ignition event was registered in the case when the visible glow was observed on the surface or in the bulk of the fuel sample. The next temperature point was chosen by the half division method [32].

3. Results

3.1. Ignition Characteristics of the Fuel Samples

Figure 3 shows the temperature dependencies of the ignition delay time measured for the samples of anthracite and semi-coke modified with various additives in a temperature range of 600–800 °C (with a step of 50 °C).
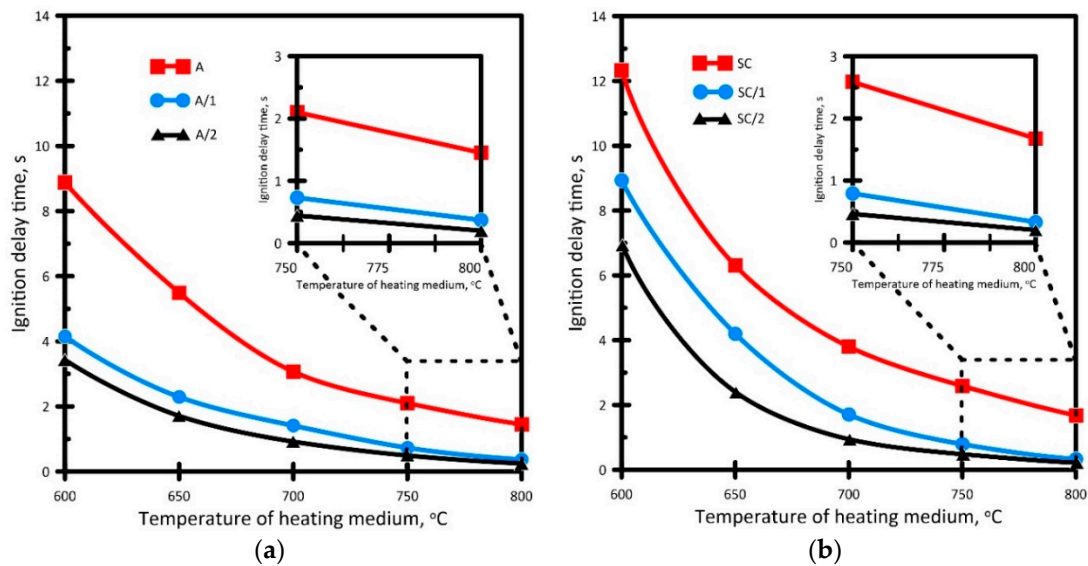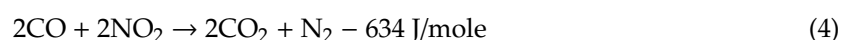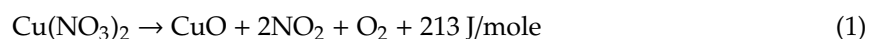
Figure 3. The dependencies of the ignition delay time on the temperature of heating medium for the samples of anthracite (**a**) and semi-coke (**b**).

One can see from Figure 3 that with a rise in the heating medium temperature (from 600 to 800 °C), the ignition delay time was decreased for all the studied samples (by 6.1 and 7.4 times for samples A for SC, respectively). The obtained curves are characterized by an exponential dependence. The different values of the ignition delay time for anthracite and semi-coke at similar temperatures could be caused by differences in the composition of the samples.

Thus, an introduction of the additives resulted in a significant reduction in the ignition delay time. The largest change in this parameter was observed in the case of the copper acetate additive. The average values of the relative change in the parameter Ti for the anthracite and semi-coke samples modified with $Cu(CH_3COO)_2$ were 73% and 70%, respectively. For samples A and SC modified with the copper nitrate, ΔTi values were 61% and 53%, respectively. Based on the obtained results, one can conclude that $Cu(CH_3COO)_2$ is the most active promotor for the combustion process. It is worth mentioning that the rise in the heating temperature (from 600 to 800 °C) caused an increase in activity of the used additives (expressed in a relative change in the ignition delay time between the original and modified samples)—by 1.4 and 2.5 times for A- and SC-series, respectively.

The major reasons for the promotion of the combustion process seem to be an involvement of the solid and gaseous products of the salts' decomposition into the ignition stage, as well as the thermal effects of these processes. Various additives had different activating mechanisms corresponding to their chemical nature. For instance, the possible mechanism of the copper nitrate action includes the following chemical reactions:

$$Cu(NO_3)_2 \rightarrow CuO + 2NO_2 + O_2 + 213 \text{ J/mole} \tag{1}$$

$$2Cu(NO_3)_2 + 3C \rightarrow 2CuO + 4NO + 3CO_2 - 923 \text{ J/mole} \tag{2}$$

$$C + NO_2 \rightarrow CO + NO - 54 \text{ J/mole} \tag{3}$$

$$2CO + 2NO_2 \rightarrow 2CO_2 + N_2 - 634 \text{ J/mole} \tag{4}$$

$$NO + 1/2O_2 \rightleftarrows NO_2 - 57 \text{ J/mole} \tag{5}$$

$$C + O_2 \rightarrow CO_2 - 394 \text{ J/mole} \tag{6}$$

The initial stage implies the decomposition of $Cu(NO_3)_2$ (1) with the consequent formation of nitrogen oxides (2) and (3). The NO_2 species (5) formed during the decomposition can act as a

strong oxidizing agent for the combustion of fuel carbon (3) and released volatile substances (4) [33]. In this case, carbon could serve as a reducing reagent (reaction 2), accelerating the salt decomposition process. The interaction of the residual carbon with air oxygen is described by the reaction (6) and is accompanied by the further oxidation of the nitrogen oxide.

The decomposition of $Cu(NO_3)_2$ results in the appearance of the dispersed non-stoichiometric copper oxide, which may be composed of different CuO_x phases. Further oxidation of copper species predominantly results in the formation of a single copper oxide phase CuO, which is known to be a very active catalyst for heterogeneous oxidation reactions (6) [34]. The emergence of the dispersed CuO is assumed to exert an additional promoting effect on the anthracite and semi-coke combustion.

In atmospheric air, the copper acetate decomposition is followed by the complete oxidation of the released products to form carbon dioxide and water, according to the following gross reaction (7):

$$Cu(CH_3COO)_2 + 4O_2 \rightarrow CuO + 4CO_2 + 3H_2O - 1583 \text{ J/mole} \qquad (7)$$
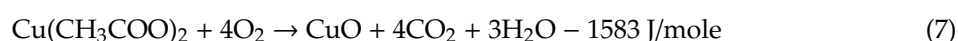
The decomposition of $Cu(CH_3COO)_2$ accompanied by the oxidation of the released products has a very strong exothermal effect [35,36], which, in turn, provokes the earlier release of the volatile compounds from the fuel. As a result, the observed ignition delay time tends to be reduced for the modified samples.

It is worth noting that the observed change in the ignition delay time of the activated anthracite and semi-coke samples could be associated with an increase in the O/C ratio (Table 2).

Figure 4 compares the determined values of the minimum ignition temperature for the studied samples.
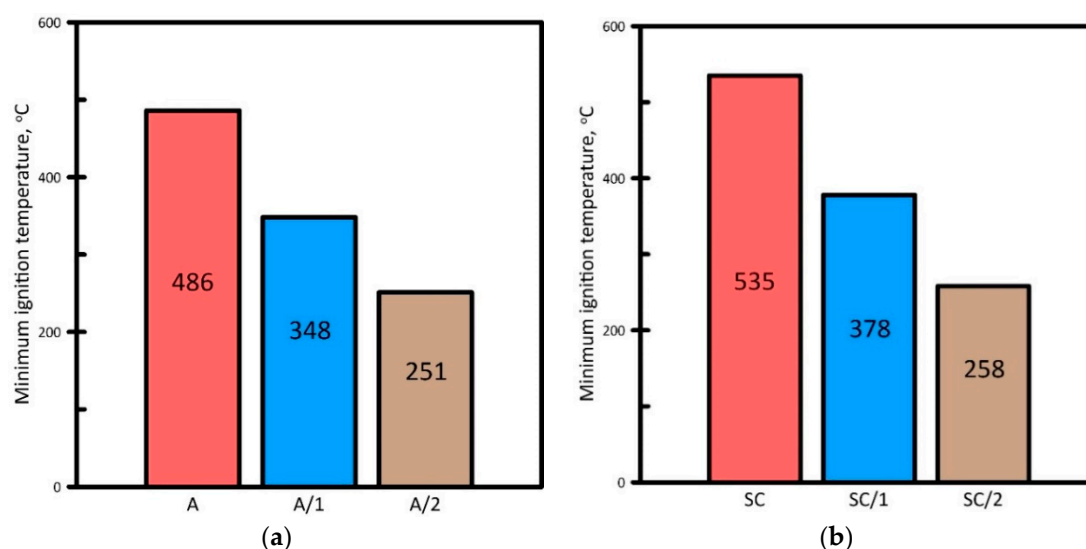
Figure 4. The dependencies of the ignition delay time on the temperature of heating medium for the samples of anthracite (**a**) and semi-coke (**b**).

The highest ignition temperature was characteristic for the reference SC sample (T_{min} = 535 °C), which is presumably associated with the minimum content of volatile matter and high carbon content in terms of the dry ash-free mass of the sample (Tables 1 and 2). For the reference A sample, T_{min} was as high as 486 °C. The introduction of the activating additives led to a significant decrease in the minimum ignition temperature (from 138 to 277 °C). In this case, the highest values of T_{min} (235 °C and 277 °C) were observed for the samples modified with copper acetate (A/2 and SC/2, respectively). It is worth mentioning that for the sample with high carbon content (SC), the activating effect of the additive was the most expressed. The observed result is in good agreement with the data reported in the literature [5,7]. This was explained by the fact that the coal surface possesses the active O-containing

functional groups [29]. The higher the coalification degree of fuel, the lower the content of O-groups, which is illustrated by the results of the elemental analysis presented in Table 2.

3.2. Combustion Characteristics of the Fuel Samples

The characteristic images of the ignition and subsequent combustion stages for the studied samples are given in Figures 5 and 6 for the anthracite and semi-coke series, accordingly.
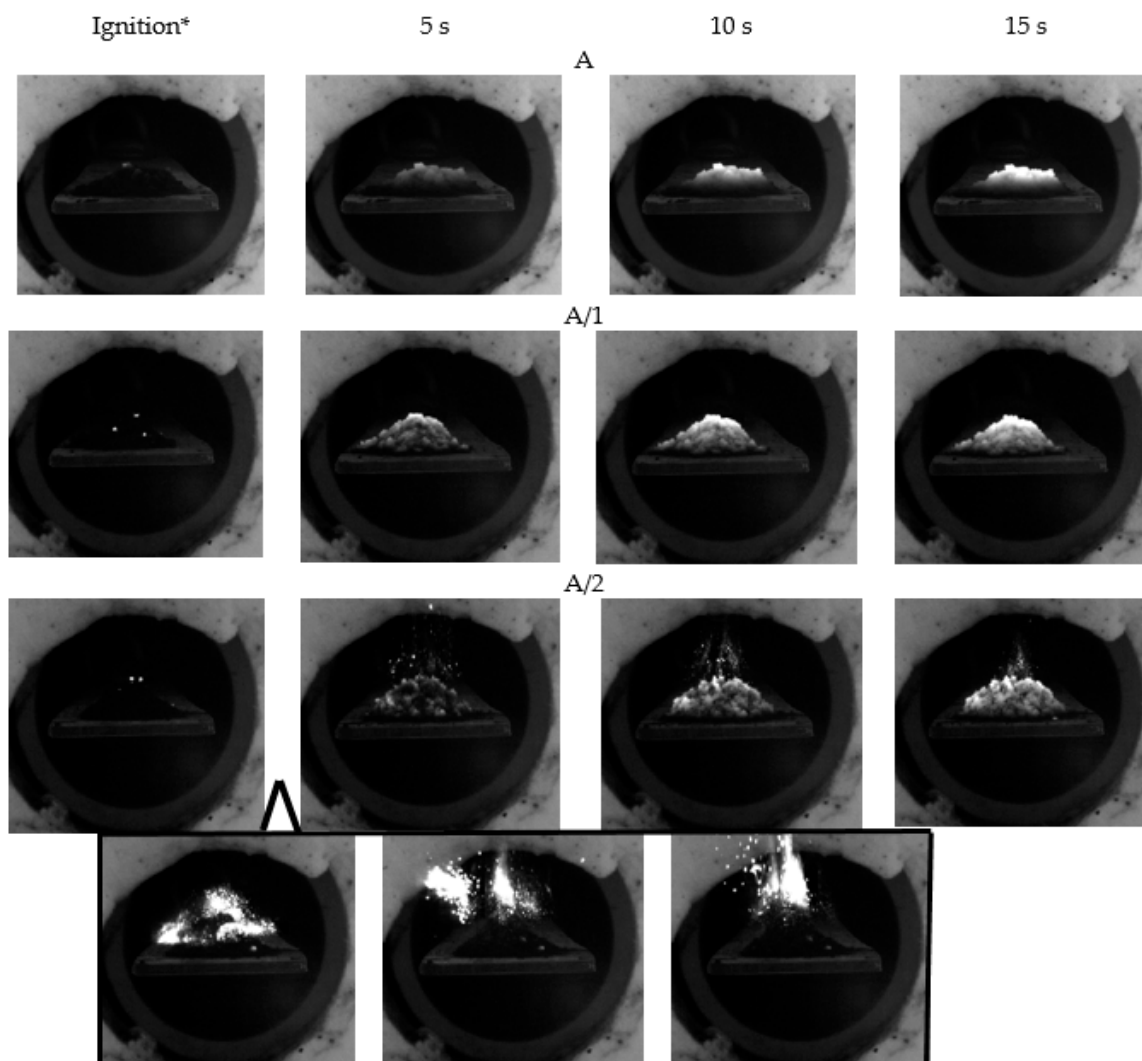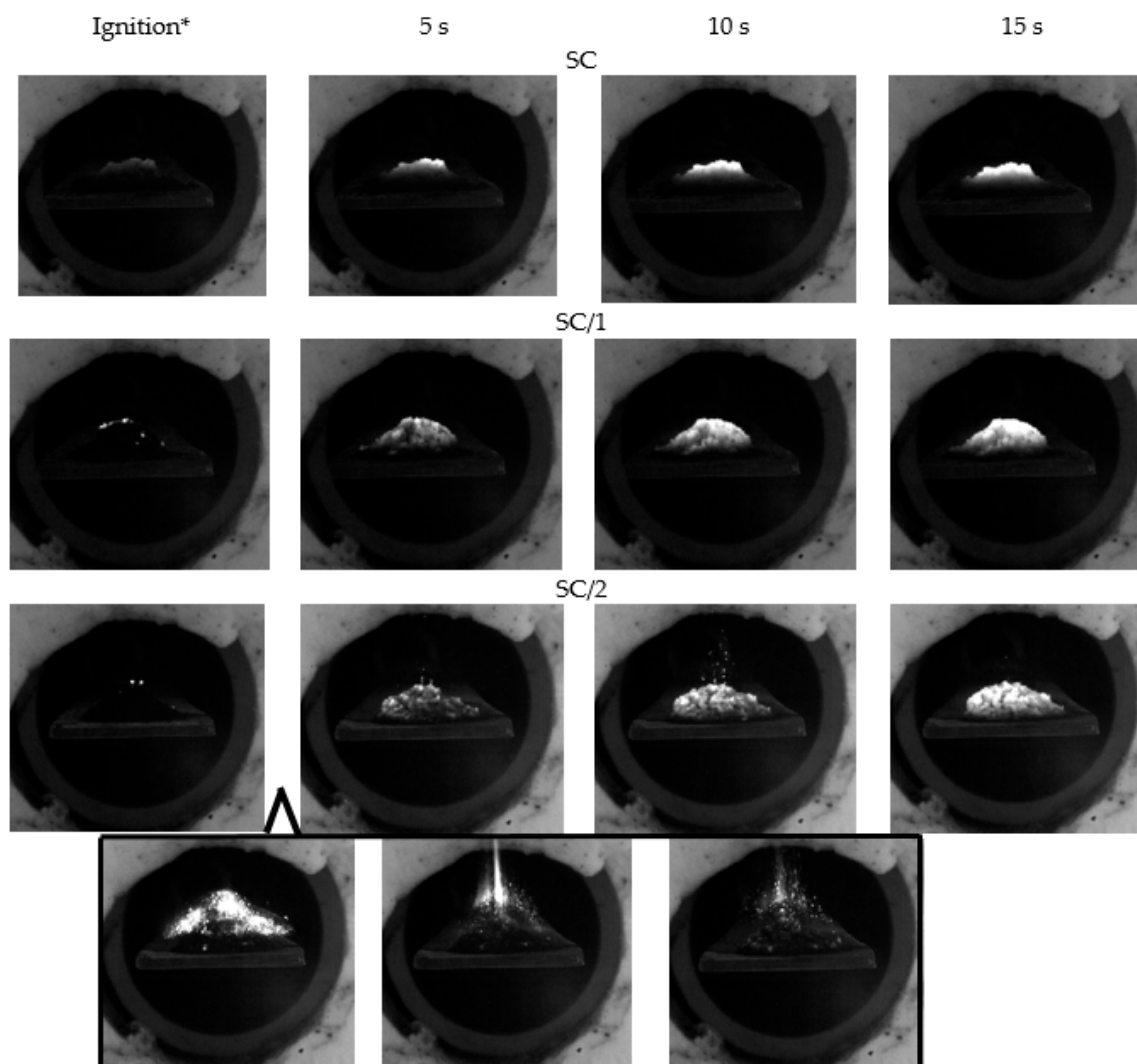

Figure 5. The ignition and subsequent combustion of the A-series samples at a heating medium temperature of 800 °C. (* Ignition delay time: A—1.5 s, A/1—0.4 s, A/2—0.2 s).

The physical model of the ignition and subsequent combustion processes comprises a set of consecutive and parallel stages: the heating and the moisture evaporation; the thermal destruction of the samples and the beginning of the volatile matter release; the mixing of the combustible gases (including the gas-phase decomposition products of the deposited additives) with an oxidizing medium; and the thermal decomposition of the carbon residue in a flameless combustion regime in the presence of catalytically active copper oxide [34].

In the case of the samples modified by $Cu(NO_3)_2$, such a combustion regime at the initial stage was caused by the low content of the volatile matter (Table 1). For the reference samples A and SC, with the expiration of the residence time (from the moment of ignition) under the conditions of the air heating, the propagation of the combustion front from the surface to the center of the specimen was

observed without a pronounced zone of local ignition. Later (in the time interval between 5 and 10 s), the glow intensity was increased, which is explained by an increase in the combustion temperature [37]. At the same time, for the A sample, in contrast to the SC sample, a more intense propagation of the combustion front was observed, which could be associated with a higher content of the volatile matter in the composition of this sample (Table 1). Thus, the release of a larger amount of volatiles at an early stage of the thermal transformation of the sample is thought to promote the oxidation and propagation of the combustion front.

Figure 6. The ignition and subsequent combustion of SC series samples at a heating medium temperature of 800 °C. (* Ignition delay time: SC—1.7 s, SC/1—0.3 s, SC/2—0.2 s).

For the modified samples, along with the early ignition and decrease in the minimum temperature corresponding to this process, an intensive propagation of the combustion front was observed after the sample ignition. Presumably, this was caused by an improvement in the efficiency of the oxygen diffusion inside the porous space of the sample due to the appearance of new channels and cracks in its structure, which could be formed due to the decomposition of the activating additives within the pores of fuel particles. It was earlier found [38] that the introduction of copper-salt additives (for example, $Cu(NO_3)_2$) speeds up the volatile matter release due to the significant morphological change occurred on the particles' surface.

At the late periods of combustion, the catalytic effect of CuO [34] results in the further development of the specific surface area of the fuel particles, thus boosting the oxygen supply to the sample.

In particular, it should be noted that an additional improvement in the processes of mass transfer during the oxidation of modified samples could apparently be provided by certain micro-explosions (for samples A/2 and SC/2), which are observed at the early stage of the combustion process.

For the samples modified with copper acetate, the formation of micro-explosions was recorded during the entire time interval of the combustion process (Figures 5 and 6), which is similar to the explosions accompanying the combustion of metal powders [39]. In this case, the epicenter of the micro-explosions can be observed both from the surface and bulk of the fuel specimen. This effect could be associated with the intense release of flammable gases of the volatile matter that appeared during the thermal decomposition of the additives. Additionally, some gas-phase products of thermal decomposition of the additives in the form of carbon monoxide could also promote the ignition and combustion of the studied fuels. In this case, the peculiarity of combustion is associated with the formation of a stable visible flame near the surface of the specimen, which was formed as a result of the micro-explosions' occurrence in the early period of the combustion. The size of the observed flame was approximately two times higher than the height of the sample pile. Presumably, the formation of such a flame is related to the reactions of air oxygen with the gas-phase products of the copper acetate decomposition (vapors of acetone, acetaldehyde, and acetic acid [35,36]).

Thus, for the anthracite and semi-coke samples modified with copper acetate, the combustion process is characterized by the gas-phase ignition mechanism. It takes place as soon as the threshold concentrations and temperature of the mixture of the combustible gases evolved into the thermal decomposition of additives are reached. This effect leads to a significant change in the structure of particles facilitating the effective opening of their porous structure. Subsequently, this effect may cause a more intensive release of the volatiles and faster propagation of the combustion front.

The same can be said about the samples modified with copper nitrate. Earlier [40], it was found that the combustion of bituminous coal modified with the copper nitrate additive was accompanied by the formation of successive micro-explosions, which leads to a significant change in the shape of the fuel particles. For these samples, such pronounced effects were not observed due to the different physicochemical structure of the fuel. An exception was the change in the surface of the fuel specimen at the early stage of the fuel exposure in the combustion chamber.
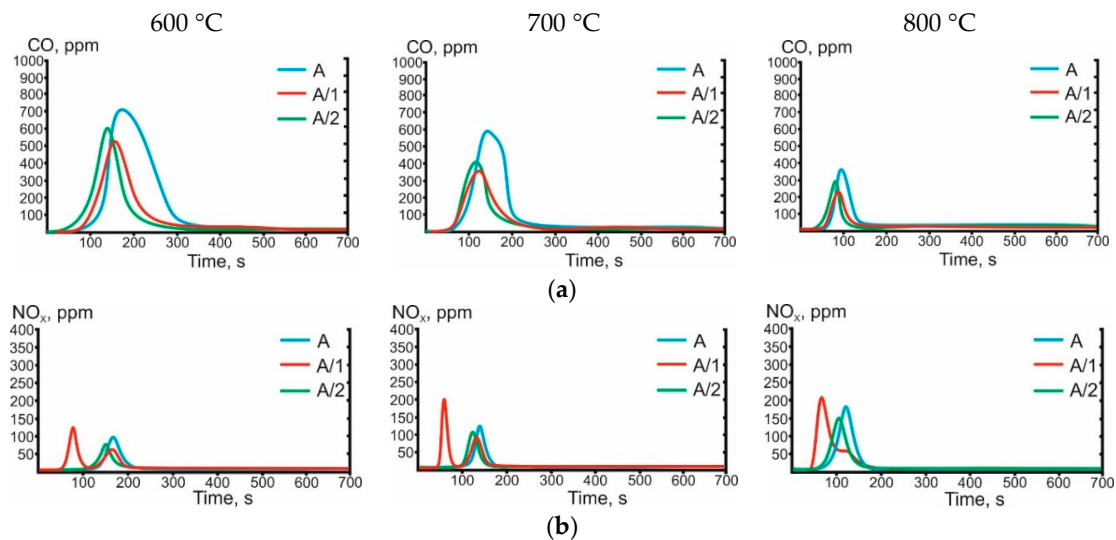
3.3. Gas-Phase Combustion Products

The main gas-phase combustion product for all the studied samples was carbon dioxide, for which the behavior profiles had a similar character with the mass loss of the fuel sample during the thermal transformation [20,21]. The differences in the formation character of other gases, CO and NO_x, are of great interest. The experimental results for anthracite and semi-coke are presented in Figures 7 and 8, respectively. For each sample, the integrand area of the CO and NO_x release curves was also calculated, thus characterizing the total amount of each gas formed. These values, as well as the ratios of the integrand areas determined for the initial and modified samples, are summarized in Table 3. Based on these data, the contribution of the activating additive to the combustion process was evaluated.

The analysis of the gas-phase combustion products revealed that the concentration profiles of CO release (Figures 7a and 8a) had a monomodal form, which may be caused by the low content of the volatile substances in the composition of the reference samples of anthracite and semi-coke (Table 1). It is worth noting that for all the samples with an increase in the temperature of the heating medium, a decrease in the amount of CO released along with a narrowing of the peak was observed. This was due to the acceleration of the CO oxidation to CO_2. On the other hand, the observed fact could also be explained by a decrease in the time interval within which the combustion of the samples occurred. The highest concentration of CO in the composition of the combustion products was obtained for the SC sample.

For the samples with the activating additives, a significant decrease in the total amount of formed CO was observed. For the modified samples, a decrease in the amount of CO was about 52% and 61% for anthracite and semi-coke, respectively (Table 3). In this case, the CO concentration profiles for

the modified samples were characteristically shifted to the left along the time scale. The maximum decrease in the amount of CO was observed in the case of using copper nitrate (samples A/1 and SC/1). Despite the fact that the greatest effect in lowering the temperature and ignition delay times of anthracite and semi-coke was obtained in the case of $Cu(CH_3COO)_2$ additive (Figures 3 and 4), the maximum CO concentrations for these samples were intermediate. Apparently, this was due to the appearance of an additional amount of CO derived from the copper acetate thermal decomposition [36].

Figure 7. The concentration profiles for the gaseous products formation during the combustion of the studied anthracite samples at different temperatures of heating medium: (**a**) CO; (**b**) NO_x.
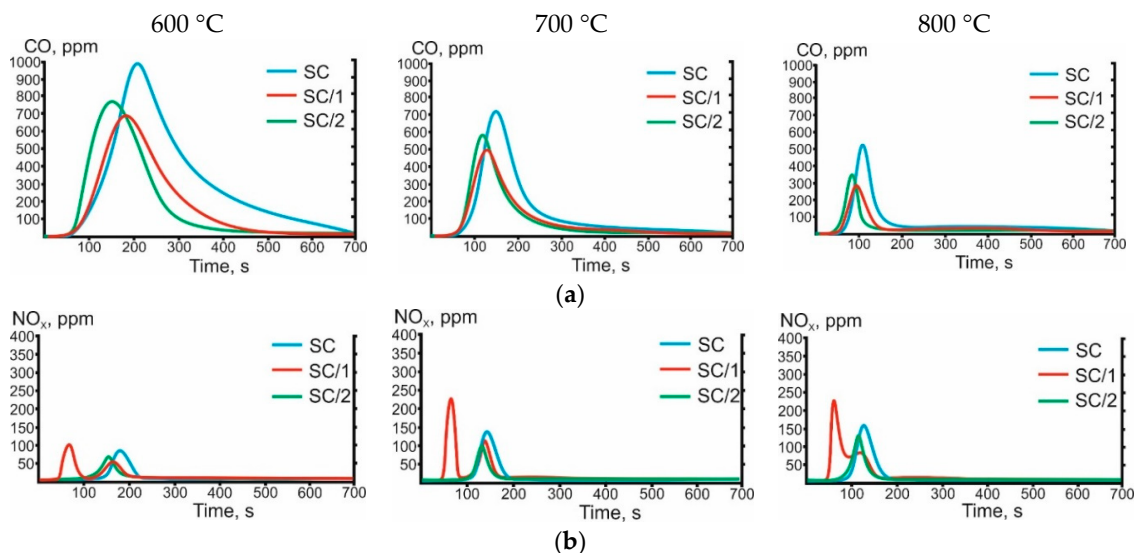
Figure 8. The concentration profiles for the gaseous products formation during the combustion of the studied semi-coke samples at different temperatures of heating medium: (**a**) CO; (**b**) NO_x.

The formation of NO_x during the fuel combustion was associated with the high-temperature oxidation of nitrogen contained in the fuel and atmospheric air. A decrease in concentration maxima, as well as in the total amount of emitted NO_x (by 35 % on average) for the studied samples modified with copper acetate can be explained by a certain decrease in the nitrogen content in the fuel (Table 2) and a lesser involvement of the molecular nitrogen from the air in the oxidation processes. On the other hand, in the case of combustion of the modified A/1 and SC/1 samples, the process was accompanied by the additional formation of nitrogen oxide due to the apparent decomposition of copper nitrate [31].

According to the data presented in Table 3, the rise in T_g temperature leads to a decrease in the S^{CO}_{MS}/S^{CO}_{ref} ratio. This fact could be explained by the enhancement of the additive's activating properties at higher temperatures, which is consistent with the results of our previous work [21]. At the same time, the greatest decrease in the amount of CO was obtained for samples modified with copper nitrate (in particular, for sample SC/1).

Table 3. Relative integrand area of peaks related to CO an NO_x release for the initial (S^{CO}_{ref} and S^{NOx}_{ref}) and modified (S^{CO}_{MS} and S^{NOx}_{MS}) samples.

Sample	Temperature of Heating Medium, °C					
	600	700	800	600	700	800
	S^{CO}_{MS}/S^{CO}_{ref}			$S^{NOx}_{MS}/S^{NOx}_{ref}$		
A/1	0.58	0.52	0.48	1.63	1.49	1.06
A/2	0.81	0.59	0.56	0.60	0.66	0.74
SC/1	0.72	0.58	0.39	1.45	1.27	1.03
SC/2	0.82	0.63	0.43	0.53	0.60	0.73

4. Conclusions

In the present work, the promoting effect of two different copper salt additives, $Cu(NO_3)_2$ and $Cu(CH_3COO)_2$, on the character of the anthracite and semi-coke combustion was investigated. The results of determining the minimum temperature of ignition and the ignition delay time of fuels allow us to conclude that the $Cu(CH_3COO)_2$ additive made the greatest contribution to the activation of the ignition process. In the case of using this additive for the anthracite sample, the minimum ignition temperature decreased to 235 °C, and for the semi-coke sample, this value was 277 °C. The difference in the obtained values is associated with a lower content of the volatile matter and oxygen-containing functional groups present in the composition of the semi-coke sample. The reduction in the ignition delay time for the samples modified with copper salts varied in a range from 50 to 70%.

The flameless regime of the combustion of the sample at the initial stage of fuel heating was observed via a high-speed video camera. For the samples modified with Cu-containing additives, the more intense flame accompanied by the micro-explosions was observed (at the early stage of combustion). These micro-explosions were derived from the thermal deformation of the fuel particles with the simultaneous development of their porous structure. As a result, a relatively large volume of combustible gases was released, including the decomposition products of the introduced additives.

The composition of the gas-phase combustion products indicated the significant effect of the copper salt additives, allowing one to decrease the CO concentration in the released gases with a characteristic shift of CO-release peak to the earlier time period. Copper acetate facilitated a decrease in the concentration of releasing nitrogen oxides (by 35% on average at different heating medium temperatures) formed from atmospheric nitrogen during the coal combustion.

The results of this study expand our understanding of the possibilities of changing the reactivity of fuels with a high coalification degree and provide new data on the features of their combustion in the presence of copper salt activating additives. The revealed regularities of activated combustion could also be further applied for the development of more effective combustion methods for solid fuels with low reactivity, providing higher burnout and improving the environmental characteristics of the released gaseous combustion products.

Author Contributions: Conceptualization, I.M. and A.V.; methodology, K.L., S.T. and Y.B.; validation, K.L.; formal analysis, K.L.; writing—original draft preparation, K.L. and K.S.; writing—review and editing, I.M., A.V. and A.G.; visualization, A.T.; project administration, A.G.; funding acquisition, A.G. All authors have read and agreed to the published version of the manuscript.

References

1. Köpsel, R.F.W.; Halang, S. Catalytic influence of ash elements on NO_x formation in char combustion under fluidized bed conditions. *Fuel* **1997**, *76*, 345–351. [CrossRef]

2. Statistical Review of World Energy. 2020. Available online: https://www.bp.com/content/dam/bp/business-sites/en/global/corporate/pdfs/energy-economics/statistical-review/bp-stats-review-2020-full-report.pdf (accessed on 17 September 2020).

3. Ma, Z.; Deng, J.; Li, Z.; Li, Q.; Zhao, P.; Wang, L.; Sun, Y.; Zheng, H.; Pan, L.; Zhao, S.; et al. Characteristics of NO_x emission from Chinese coal-fired power plants equipped with new technologies. *Atmos. Environ.* **2016**, *131*, 164–170. [CrossRef]

4. Zou, C.; Zhao, J.; Li, X.; Shi, R. Effects of catalysts on combustion reactivity of anthracite and coal char with low combustibility at low/high heating rate. *J. Therm. Anal. Calorim.* **2016**, *126*, 1469–1480. [CrossRef]

5. Gong, X.; Guo, Z.; Wang, Z. Reactivity of pulverized coals during combustion catalyzed by CeO_2 and Fe_2O_3. *Combust. Flame* **2010**, *157*, 351–356. [CrossRef]

6. Gong, X.-Z.; Guo, Z.-C.; Wang, Z. Anthracite combustion catalyzed by Ca-Fe-Ce series catalyst. *Ranliao Huaxue Xuebao J. Fuel Chem. Technol.* **2009**, *37*, 421–426.

7. Gong, X.; Guo, Z.; Wang, Z. Variation on anthracite combustion efficiency with CeO_2 and Fe_2O_3 addition by Differential Thermal Analysis (DTA). *Energy* **2010**, *35*, 506–511. [CrossRef]

8. Gong, X.; Zhang, S. Catalytic Effects of CeO_2/Fe_2O_3 and Inherent Mineral Matter on Anthracite Combustion Reactions and Its Kinetic Analysis. *Energy Fuels* **2017**, *31*, 12867–12874. [CrossRef]

9. Yazykov, N.A.; Simonov, A.D.; Dubinin, Y.V.; Zaikina, O.O. Catalytic Co-Combustion of Peat and Anthracite in a Fluidized Bed. *Catal. Ind.* **2019**, *11*, 342–348. [CrossRef]

10. Yang, L.; Luo, H.; Zhang, K.; Gong, Z.; Wu, W. Effect of limonite additive on combustion and NO_x emission characteristics of anthracite. *Meitan Xuebao J. China Coal Soc.* **2019**, *44*, 305–312.

11. Gong, X.Z.; Guo, Z.C.; Wang, Z. Effect of K_2CO_3 and Fe_2O_3 on combustion reactivity of pulverized coal by thermogravimetry analysis. *Ranliao Huaxue Xuebao J. Fuel Chem. Technol.* **2009**, *37*, 42–48.

12. Betancur, Y.; López, D.; Du, Z.-Y.; Li, W.-Y. The role of K_2CO_3 on structural changes of coal, biomass and coal/biomass blends during pre-treatment using N_2 and CO_2. Differences in the reactivity under oxy-combustion conditions. In Proceedings of the 2018 International Pittsburgh Coal Conference The Thirty-Fifth Annual Pittsburgh Coal Conference, Xuzhou, China, 15–18 October 2018.

13. Cheng, J.; Zhou, F.; Xuan, X.; Liu, J.; Zhou, J.; Cen, K. Cascade chain catalysis of coal combustion by Na–Fe–Ca composite promoters from industrial wastes. *Fuel* **2016**, *181*, 820–826. [CrossRef]

14. Zou, C.; Wen, L.; Zhang, S.; Bai, C.; Qiu, G.; Lü, X.; Tan, X. Effects of catalysts on the conbustion behavior of pulverized coal injection (PCI) anthracite and its mechanism. *Metal Int.* **2011**, *16*, 53–60.

15. Belyaev, A.A. Effect of alkali metal carbonate additives on the rate of oxidation of the organic matter of anthracite. *Solid Fuel Chem.* **2013**, *47*, 226–230. [CrossRef]

16. Sen, K.; Dash, P.S. Quantum chemical perspective of coal molecular modeling: A review. *Fuel* **2020**, *279*, 118539. [CrossRef]

17. Gong, X.; Guo, Z.; Wang, Z. Experimental study on mechanism of lowering ignition temperature of anthracite combustion catalyzed by Fe_2O_3. *Huagong Xuebao/CIESC J.* **2009**, *60*, 1707–1713.

18. Gong, X.Z.; Guo, Z.C.; Wang, Z. Effect of coal characteristics on its combustion catalyzed by CeO_2. *Ranliao Huaxue Xuebao J. Fuel Chem. Technol.* **2010**, *38*, 29–34.

19. Li, X.G.; Ma, B.G.; Xu, L.; Luo, Z.T.; Wang, K. Catalytic effect of metallic oxides on combustion behavior of high ash coal. *Energy Fuels* **2007**, *21*, 2669–2672. [CrossRef]

20. Larionov, K.B.; Zenkov, A.V.; Slyusarsky, K.V.; Mishakov, I.V. Intensification of thermal coal and coke oxidation by metal oxides and their precursors. *J. Phys. Conf. Ser.* **2020**, *1565*, 012037. [CrossRef]

21. Larionov, K.B.; Mishakov, I.V.; Slyusarskiy, K.V.; Vedyagin, A.A. Intensification of bituminous coal and lignite oxidation by copper-based activating additives. *Int. J. Coal Sci. Technol.* **2020**, in press. [CrossRef]

22.	Chai, Y.F.; Ning, X.J.; Zhang, J.L.; Qi, C.L.; Li, F.G.; Wang, S. Study on pulverized coal combustion catalyzed by CeO_2 under different heating rates. *Chin. Rare Earths* **2014**, *35*, 1–6.

23.	Zhang, S.; Chen, Z.D.; Chen, X.J.; Gong, X.Z. Effects of ash/K_2CO_3/Fe_2O_3 on ignition temperature and combustion rate of demineralized anthracite. *Ranliao Huaxue Xuebao J. Fuel Chem. Technol.* **2014**, *42*, 166–174. [CrossRef]

24.	Zhu, Q. Effect of calcium-based composite additives on combustion and sulfur retention of an anthracite coal. *Chin. J. Environ. Eng.* **2014**, *8*, 5413–5418.

25.	Zhou, H.; Liu, R.P.; Liu, Z.H.; Cheng, M.; Cen, K.F. Influence of alkali metal on the evolution of NO_x during coke combustion. *Meitan Xuebao J. China Coal Soc.* **2015**, *40*, 1160–1164.

26.	Dong, L.; Han, S.; Yu, W.; Lei, Z.; Kang, S.; Zhang, K.; Yan, J.; Li, Z.; Shui, H.; Wang, Z.; et al. Effect of volatile reactions on the yield and quality of tar from pyrolysis of Shenhua bituminous coal. *J. Anal. Appl. Pyrolysis* **2019**, *140*, 321–330. [CrossRef]

27.	Larionov, K.B.; Gromov, A.A. Non-isothermal oxidation of coal with $Ce(NO_3)_3$ and $Cu(NO_3)_2$ additives. *Int. J. Coal Sci. Technol.* **2019**, *6*, 37–50. [CrossRef]

28.	Tokareva, I.V.; Mishakov, I.V.; Vedyagin, A.A.; Korneev, D.V.; Petuhkova, E.S.; Savvinova, M.E. Modification of carbon fibers forrein forcingpipe polyethylene. *Compos. Nanostruct.* **2014**, *6*, 158–167.

29.	Zhang, L.; Hu, S.; Chen, Q.; Xiao, L.; Shatir, A.; Syed-Hassan, S.S.A.; Jiang, L.; Wang, Y.; Su, S.; Xiang, J. Molecular structure characterization of the tetrahydrofuran-microwave-extracted portions from three Chinese low-rank coals. *Fuel* **2017**, *189*, 178–185. [CrossRef]

30.	Liu, J.; Luo, L.; Ma, J.; Zhang, H.; Jiang, X. Chemical properties of superfine pulverized coal particles. 3. Nuclear magnetic resonance analysis of carbon structural features. *Energy Fuels* **2016**, *30*, 6321–6329. [CrossRef]

31.	Wayne, H.R. *Copper Compounds. Ullmann's Encyclopedia of Industrial Chemistry*; Wiley-VCH: Weinheim, Germany, 2005.

32.	Kramer, H. *Mathematical Methods of Statistics*; Almquist and Wiskell: Stockholm, Sweden, 1975.

33.	Wang, Y.; Wang, J.; Chen, H.; Yao, M.; Li, Y. Preparation and NOx-assisted soot oxidation activity of a CuO–CeO_2 mixed oxide catalyst. *Chem. Eng. Sci.* **2015**, *135*, 294–300. [CrossRef]

34.	Chen, L.; Li, L.; Li, G. Synthesis of CuO nanorods and their catalytic activity in the thermal decomposition of ammonium perchlorate. *J. Alloys Compd.* **2008**, *464*, 532–536. [CrossRef]

35.	Arii, T.; Masuda, Y. Thermal decomposition of calcium copper acetate hexahydrate by simultaneous measurement of controlled-rate thermogravimetry and mass spectrometry (CRTG-MS). *Thermochim. Acta* **1999**, *342*, 139–146. [CrossRef]

36.	Zhang, K.; Hong, J.; Cao, G.; Zhan, D.; Tao, Y.; Cong, C. The kinetics of thermal dehydration of copper(II) acetate monohydrate in air. *Thermochim. Acta* **2005**, *437*, 145–149. [CrossRef]

37.	Glushkov, D.O.; Paushkina, K.K.; Shabardin, D.P. Co-combustion of coal processing waste, oil refining waste and municipal solid waste: Mechanism, characteristics, emissions. *Chemosphere* **2020**, *240*, 124892. [CrossRef]

38.	Larionov, K.B.; Mishakov, I.V.; Gromov, A.A. Research of thermal destruction dynamics of coal particles in oxidizing medium with copper nitrate. *J. Phys. Conf. Ser.* **2018**, *1128*, 012070. [CrossRef]

39.	Gao, W.; Zhang, X.; Zhang, D.; Peng, Q.; Zhang, Q.; Dobashi, R. Flame propagation behaviours in nano-metal dust explosions. *Powder Technol.* **2017**, *321*, 154–162. [CrossRef]

40.	Larionov, K.B.; Mishakov, I.V.; Slyusarsky, K.V. Influence of inorganic salt on the characteristics of oxidation, ignition and combustion of bituminous coal. *J. Phys. Conf. Ser.* **2019**, *1359*, 012058. [CrossRef]